Linewidths of the 0-0 hyperfine transition in optically pumped alkali-metal vapors

J. C. Camparo and R. P. Frueholz
Chemistry and Physics Laboratory, The Aerospace Corporation, P.O. Box 92957, Los Angeles, California 90009
(Received 13 July 1984)

A generalized model for the magnetic resonance signal corresponding to the 0-0 hyperfine transition in an optically pumped alkali-metal vapor is presented. Under conditions of microwave power broadening, the model predicts "anomalous" light broadening and "anomalous" relaxation narrowing of the magnetic resonance linewidth. Good agreement between theory and experiment was obtained in an experiment that confirmed the prediction of anomalous light broadening. These results show that the 0-0 hyperfine transition cannot be described as a simple two-level system; rather, the alkali-atom's nuclear spin plays an important role in determining the magnetic resonance linewidth.

I. INTRODUCTION

When considering the 0-0 hyperfine transition in an optically pumped alkali-metal vapor it is often convenient to describe the alkali-metal atom as a two-level atom. In this approximation it is quite easy to show that the magnetic resonance line shape, detected as a change in the levels' population difference, is a Lorentzian of half-width

$$\Delta_{1/2}=[(1/T_2)^2+(T_1/T_2)\omega_1^2]^{1/2} \quad (1)$$

where T_1 and T_2 are the familiar longitudinal and transverse relaxation times and ω_1 is the microwave Rabi frequency.[1] In the case of optical pumping, however, these relaxation times depend on the photon absorption rate B as well as phenomenological collisional relaxation rates γ_1 and γ_2: $1/T_1=B/2+\gamma_1$, $1/T_2=B/2+\gamma_2$.[2] Since the ratio T_1/T_2 alters the magnitude of the power-broadened linewidth, for the present discussion we will define this ratio as a linewidth enhancement factor (LEF).[3] Thus in the two-level-atom approximation the LEF is light-intensity dependent, varying from γ_2/γ_1 to unity as the light intensity increases from a very low to a very high value, and this then implies a light-intensity dependence of the microwave power-broadened linewidth.

However, in addition to the two-level-atom approximation, one usually assumes that the duration of the relaxation collisions is relatively short, in which case $\gamma_1=\gamma_2$.[4] The significance of this additional assumption is that T_1/T_2 becomes independent of the light intensity, having the constant value of unity. Thus, with the two approximations there is no dependence of the microwave power-broadened linewidth on light intensity, except negligibly through the term $(1/T_2)^2$.

Magnetic resonance in optically pumped alkali-metal vapors, however, differs from the two-level approximation in two important respects. In the first place the observable in an optical-pumping experiment is not necessarily the population difference between two levels, and in the second the strong hyperfine interaction results in two multiplets rather than two nondegenerate states. These considerations in the case of the 0-0 hyperfine transition result in the conclusion that $T_1\neq T_2$, though their ratio is approximately unity.[5] Thus, if one were to assume that Eq. (1) was reasonably correct as long as the more realistic values of T_1 and T_2 were used, one might predict a slight light-intensity dependence for the microwave power-broadened linewidth.

In the present work we show that this procedure for determining the 0-0 linewidth is grossly in error. Specifically, we find that though the linewidth can be cast in a form similar to Eq. (1), the resulting LEF is a complicated function of the degeneracies of the two hyperfine multiplets, the photon absorption rate, and the phenomenological relaxation rates γ_1 and γ_2. Contrary to what one would predict for T_1/T_2, the correct LEF has a strong light-intensity dependence and can result in a power-broadened linewidth orders of magnitude greater than the microwave Rabi frequency.

II. THEORY

A. The Vanier model

Consider a typical alkali-metal atom with nuclear spin I. As a result of the hyperfine interaction between the nuclear and valence-electron magnetic moments, the atomic ground state is split into two hyperfine sublevels characterized by a total angular momentum quantum number F. As a particular example of an alkali-metal atom's structure, Fig. 1 shows the low-lying energy levels of ^{87}Rb($I=\frac{3}{2}$). (Important atomic parameters of some other stable alkali-metal isotopes are collected in Table I.) In the vector model of the atom the total angular momentum is formed by the vector addition of the nuclear and electronic spin vectors. Following the standard nomenclature,[6] we label the two resulting eigenvalues a and b, $F=a=(I+\frac{1}{2})$ and $F=b=(I-\frac{1}{2})$, these hyperfine sublevels are separated by a frequency interval $\Delta\nu_{\rm hfs}=A(I+\frac{1}{2})$, where A is a measure of the hyperfine interaction strength. In the absence of external perturbations the two hyperfine sublevels have degeneracies $g_a=2(I+1)$ and $g_b=2I$, so that the total ground-state degeneracy is $g=2(2I+1)$. However, in a weak static magnetic field H_0, defining the z axis of a coordinate sys-

 ©1985 The American Physical Society

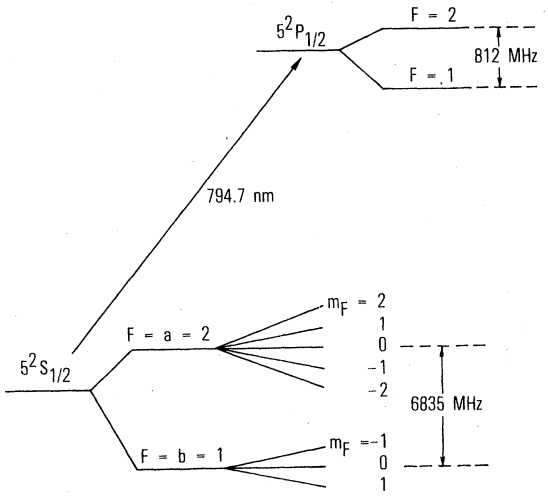

FIG. 1. The figure shows the low-lying energy levels of ^{87}Rb, not drawn to scale. Due to the combination of Doppler and pressure broadening, the excited-state hyperfine splitting was barely resolved experimentally.

tem, this degeneracy is lifted. The quantized projection of the total angular momentum on the z axis is then characterized by an additional quantum number m_F. Since the gyromagnetic ratios (g factors) of the two hyperfine multiplets are, to a good approximation, equal but of opposite sign,[7] the resulting Zeeman sublevels within each hyperfine multpilet are shifted by $\nu_L=(m_F g_F \mu_B H_0)/h$, where g_F and μ_B are the g factor and Bohr magneton, respectively. Thus, for alkali-metal atoms with noninteger nuclear spin the two hyperfine multiplets each contain a state with $m_F=0$, which to first order is unperturbed by the presence of an external magnetic field.

In this section we want to obtain an expression for the linewidth of the ground-state 0-0 hyperfine transition in an alkali-metal atom as observed in typical gas cell optical-pumping experiments. We assume that depopulation pumping by frequency-selected light creates a population imbalance between the two ground-state hyperfine multiplets, and a resonant microwave field is detected either by an increase in atomic fluorescence or a decrease in transmission of the optical-pumping light. Specifically, we are interested in the effect of the nuclear spin, manifested in the different degeneracies of the two hyperfine multiplets, on the microwave power broadening of the 0-0 transition. In order to obtain this expression we generalize a ^{87}Rb 0-0 hyperfine line-shape model, developed by Vanier and colleagues,[8,9] to the case of arbitrary noninteger nuclear spin ($I \geq \frac{3}{2}$). The key to this generalization lies in the fact that the symmetry of the Vanier model extends to any alkali-metal atom of noninteger nuclear spin: no matter what the actual ground-state degeneracy, the 0-0 hyperfine line shape is obtained by the solution of only five coupled differential equations.

To simplify our analysis we imagine a laser tuned to an optical transition for one of the ground-state hyperfine

TABLE I. Some atomic parameters of the stable alkali-metal-atom isotopes exhibiting the 0-0 hyperfine transition.

Alkali-metal-atom	I	$\Delta\nu_{\rm hfs}$ (MHz)	g	g_a	g_b
^{7}Li	$\frac{3}{2}$	804	8	5	3
^{23}Na	$\frac{3}{2}$	1772	8	5	3
^{39}K	$\frac{3}{2}$	462	8	5	3
^{41}K	$\frac{3}{2}$	254	8	5	3
^{85}Rb	$\frac{5}{2}$	3036	12	7	5
^{87}Rb	$\frac{3}{2}$	6835	8	5	3
^{133}Cs	$\frac{7}{2}$	9193	16	9	7

multiplets. Furthermore, we assume that the laser interacts with all the Zeeman sublevels of this multiplet equally, so that the optical excitation can be described by one photon absorption rate B. For an optically thin vapor the signal $S(\Delta)$ (either transmission or fluorescence) is then proportional to the increased population of the optically excited multiplet caused by a microwave field near the 0-0 hyperfine resonance. Letting η be the fraction of atoms in the absorbing multiplet, we have

$$S(\Delta)=\eta_\Delta-\eta_\infty\ , \tag{2}$$

where the subscript indicates the degree of detuning of the microwaves from the atomic resonance (i.e., $\Delta=\omega-\omega_0$, where ω is the microwave field frequency and ω_0 is the 0-0 resonance frequency). In terms of the ground-state density matrix elements,

$$\eta=\sum_{\tilde{m}_F}\rho(\tilde{F},\tilde{m}_F)\ , \tag{3}$$

where the tilde distinguishes the optically excited ground-state hyperfine multiplet, and we define the nomenclature for the density matrix elements:

$$\begin{aligned}\rho(F,m_F)&=\delta_{FF'}\delta_{m_F m_F'}\rho(F,m_F;F',m_F')\\&=\delta_{FF'}\delta_{m_F m_F'}\langle F,m_F\,|\,\rho\,|\,F',m_F'\rangle\ .\end{aligned} \tag{4}$$

In the Vanier model the evolution of the ground-state density matrix is governed by three independent processes: uniform relaxation of the ground-state Zeeman sublevels,[10] the microwave interaction, and depopulation pumping;

$$\dot{\rho}=\dot{\rho}_{\rm relax}+\dot{\rho}_{\mu\lambda}+\dot{\rho}_{\rm opt}\ . \tag{5}$$

In general, Eq. (5) represents $(2I+1)(4I+3)$ simultaneous complex equations (ignoring normalization). However, with the Vanier model this number is considerably reduced. The model ignores all but one of the possible coherences (i.e., the 0-0 coherence) because the Zeeman sublevels are considered to be well resolved; thus, $2I(4I+3)$ density matrix elements can immediately be set equal to zero. Furthermore, since the model assumes that

all Zeeman sublevels relax equivalently, that within a hyperfine manifold they all interact with the optical-pumping light equally, and that there is no repopulation pumping, the following relationship holds for the diagonal density matrix elements:

$$\rho(F,m_F)=\rho(F,m_F') \tag{6}$$

for $F=a,b$ and $m_F,m_F'\neq 0$. Equation (6) represents $2I$ equations relating the diagonal density matrix elements of the $F=a$ multiplet and $2(I-1)$ equations relating the diagonal density matrix elements of the $F=b$ multiplet. Thus, this model reduces the problem of calculating the 0-0 hyperfine line shape to $[(2I+1)(4I+3)-2I(4I+3)-2I-2(I-1)]=5$ simultaneous equations for all cases of noninteger alkali-metal nuclear spin.

In light of the above discussion, it is a straightforward procedure to generalize the density matrix rate equations of the Vanier model. We thus have

$$\dot{\rho}(\tilde{F},\tilde{m}_F)=-B\rho(\tilde{F},\tilde{m}_F)+Bg^{-1}\sum_{\tilde{m}'_F}\rho(\tilde{F},\tilde{m}'_F)+\gamma_1[g^{-1}-\rho(\tilde{F},\tilde{m}_F)]\quad(\tilde{m}_F\neq 0)\ , \tag{7a}$$

$$\dot{\rho}(\tilde{F},0)=-B\rho(\tilde{F},0)+Bg^{-1}\sum_{\tilde{m}_F}\rho(\tilde{F},\tilde{m}_F)+\gamma_1[g^{-1}-\rho(\tilde{F},0)]-\omega_1\mathrm{Im}[\rho(F,0;\tilde{F},0)\exp(i\omega t)]\ , \tag{7b}$$

$$\dot{\rho}(F,0)=Bg^{-1}\sum_{\tilde{m}_F}\rho(\tilde{F},\tilde{m}_F)+\gamma_1[g^{-1}-\rho(F,0)]+\omega_1\mathrm{Im}[\rho(F,0;\tilde{F},0)\exp(i\omega t)]\ , \tag{7c}$$

$$\dot{\rho}(F,0;\tilde{F},0)=-\left[\frac{B}{2}+\gamma_2+i\omega_0\right]\rho(F,0;\tilde{F},0)+\frac{i\omega_1}{2}[\rho(\tilde{F},0)-\rho(F,0)]\exp(-i\omega t)\ , \tag{7d}$$

$$\dot{\rho}(F,m_F)=Bg^{-1}\sum_{\tilde{m}_F}\rho(\tilde{F},\tilde{m}_F)+\gamma_1[g^{-1}-\rho(F,m_F)]\quad(m_F\neq 0)\ , \tag{7e}$$

where $\gamma_1(\gamma_2)$ is the phenomenological longitudinal (transverse) relaxation rate in the "dark." Note that in the above equations we have ignored the effect of light shifts,[11] since we are only concerned with the signal line shape.

Normalizing the density matrix results in a relationship among Eqs. (7), we have

$$2\tilde{F}\dot{\rho}(\tilde{F},\tilde{m}_F)+2F\dot{\rho}(F,m_F)+\dot{\rho}(\tilde{F},0)+\dot{\rho}(F,0)=0\ . \tag{8}$$

Thus, we can express Eq. (7e) as a linear combination of Eqs. (7a)–(7d). However, since we want to determine both the real and imaginary parts of the coherence, we are still left with five coupled differential equations. To obtain the two equations for the coherence we make the standard transformation

$$\rho(F,0;\tilde{F},0)=\rho_r(F,0;\tilde{F},0)\exp(-i\omega t)\ , \tag{9}$$

where $\rho_r(F,0;\tilde{F},0)$ is a slowly varying function of time, and we use Eq. (9) in Eq. (7d). The equations for the real and imaginary parts of the coherence which result are

$$\mathrm{Re}[\dot{\rho}_r(F,0;\tilde{F},0)]=-\left[\frac{B}{2}+\gamma_2\right]\mathrm{Re}[\rho_r(F,0;\tilde{F},0)]-\Delta\mathrm{Im}[\rho_r(F,0;\tilde{F},0)]\ , \tag{10a}$$

$$\mathrm{Im}[\dot{\rho}_r(F,0;\tilde{F},0)]=-\left[\frac{B}{2}+\gamma_2\right]\mathrm{Im}[\rho_r(F,0;\tilde{F},0)]+\Delta\mathrm{Re}[\rho_r(F,0;\tilde{F},0)]+\frac{\omega_1}{2}[\rho(\tilde{F},0)-\rho(F,0)]\ . \tag{10b}$$

Equations (7a)–(7c) and Eqs. (10a) and (10b) offer a complete description of the evolution of the ground-state density matrix in the Vanier model. Expressed in matrix form,

$$\dot{\underline{\sigma}}=-\underline{\Delta}\underline{\sigma}+\underline{\lambda}\ , \tag{11}$$

where $\underline{\sigma}$ can be thought of as a "reduced" density matrix vector defined by

$$\underline{\sigma}=\begin{bmatrix}\sigma_1\\ \sigma_2\\ \sigma_3\\ \sigma_4\\ \sigma_5\end{bmatrix}=\begin{bmatrix}\rho(\tilde{F},\tilde{m}_F)(\tilde{m}_F\neq 0)\\ \rho(\tilde{F},0)\\ \rho(F,0)\\ \mathrm{Re}[\rho_r(F,0;\tilde{F},0)]\\ \mathrm{Im}[\rho_r(F,0;\tilde{F},0)]\end{bmatrix} \tag{12}$$

with

$$\underline{\Delta}=\begin{bmatrix} \frac{2B}{g}\left[\frac{g}{2}-\tilde{F}\right]+\gamma_1 & -\frac{B}{g} & 0 & 0 & 0 \\ -\frac{2\tilde{F}B}{g} & \frac{B(4I+1)}{g}+\gamma_1 & 0 & 0 & \omega_1 \\ -\frac{2\tilde{F}B}{g} & -\frac{B}{g} & \gamma_1 & 0 & -\omega_1 \\ 0 & 0 & 0 & \frac{B}{2}+\gamma_2 & \Delta \\ 0 & -\frac{\omega_1}{2} & \frac{\omega_1}{2} & -\Delta & \frac{B}{2}+\gamma_2 \end{bmatrix} \tag{13}$$

and

$$\underline{\lambda}=\gamma_1 g^{-1}\begin{bmatrix}1\\1\\1\\0\\0\end{bmatrix}. \tag{14}$$

Thus, from Eqs. (11)—(14), we have in steady state

$$\sigma_i=\gamma_1 g^{-1}\sum_{j=1}^{3}(\underline{\Delta}^{-1})_{ij}\ , \tag{15}$$

so that the fraction of atoms in the absorbing state becomes

$$\eta=2\tilde{F}\sigma_1+\sigma_2=\gamma_1 g^{-1}\sum_{j=1}^{3}[2\tilde{F}(\underline{\Delta}^{-1})_{1j}+(\underline{\Delta}^{-1})_{2j}]\ . \tag{16}$$

It is a straightforward, though tedious, task to determine $\underline{\Delta}^{-1}$ and hence η, but after a good deal of algebraic manipulation we obtain the relatively simple expression

$$\eta=\frac{g_p\gamma_1}{g_u B+g\gamma_1}\left[\frac{\Gamma_2^2+\Delta^2+(\Gamma_2/\Gamma_{1\alpha})\omega_1^2}{\Gamma_2^2+\Delta^2+(\Gamma_2/\Gamma_{1\beta})\omega_1^2}\right], \tag{17}$$

where g_p and g_u refer to the degeneracies of the optically excited and nonoptically excited ground-state hyperfine multiplets (pumped and unpumped) respectively; Γ_2 is the standard dephasing rate indicated by Eqs. (10),

$$\Gamma_2=\frac{B}{2}+\gamma_2\ , \tag{18}$$

and the two terms $\Gamma_{1\alpha}$ and $\Gamma_{1\beta}$ can be *thought of* as longitudinal relaxation rates:

$$\Gamma_{1\alpha}=\frac{g_p\gamma_1(B+\gamma_1)}{g_p(B+\gamma_1)-\tilde{F}B} \tag{19}$$

and

$$\Gamma_{1\beta}=\frac{2\gamma_1(B+\gamma_1)(g_u B+g\gamma_1)}{(g_u-1)B^2+(g+2g_u)B\gamma_1+2g\gamma_1^2}\ . \tag{20}$$

In the present context, however, $\Gamma_{1\alpha}$ and $\Gamma_{1\beta}$ are merely constructs for casting the signal line shape and linewidth into forms similar to the two-level-atom approximation. Thus, investing these rates with physical significance should be done with caution. Finally, using Eq. (17) in Eq. (2) we obtain an expression for the 0-0 line shape:

$$S(\Delta)=\frac{g_p\gamma_1}{g_u B+g\gamma_1}\left[\frac{\Gamma_2(\Gamma_{1\alpha}^{-1}-\Gamma_{1\beta}^{-1})\omega_1^2}{\Gamma_2^2+\Delta^2+(\Gamma_2/\Gamma_{1\beta})\omega_1^2}\right], \tag{21}$$

which is seen to be a Lorentzian of half-width

$$\Delta_{1/2}=[\Gamma_2^2+(\Gamma_2/\Gamma_{1\beta})\omega_1^2]^{1/2}\ . \tag{22}$$

B. Light broadening and relaxation narrowing

As with any line-shape model, one of the most intriguing predictions of the Vanier model concerns the linewidth. In particular, in the limit of high microwave Rabi frequency the 0-0 hyperfine linewidth becomes

$$\Delta_{1/2}\simeq\omega_1\sqrt{\Gamma_2/\Gamma_{1\beta}}\ , \tag{23}$$

so that the ratio $\Gamma_2/\Gamma_{1\beta}$ plays the role of a linewidth enhancement factor. Defining R as the normalized photon absorption rate, $R=B/\gamma_1$, and approximating $\gamma_1=\gamma_2$, the LEF becomes

$$\Gamma_2/\Gamma_{1\beta}=\frac{(2+R)[(g_u-1)R^2+(g+2g_u)R+2g]}{4(1+R)(g+g_u R)} \tag{24}$$

and is plotted in Figs. 2(a) and 2(b) as a function of R for several values of the nuclear spin. Several important properties of the LEF are clearly illustrated by Fig. 2 and are worth discussing in some detail.

(i) First, we note that the ratio $\Gamma_2/\Gamma_{1\beta}$ is always greater than unity. Thus, the ratio acts as a true enhancement factor, so that linewidths less than the Rabi frequency never occur.

(ii) No matter which hyperfine multiplet is optically excited, the LEF is an increasing function of nuclear spin. Thus, power broadening for Cs($I=\frac{7}{2}$) is always greater (given similar conditions) than power broadening for ^{87}Rb($I=\frac{3}{2}$). This prediction is of fundamental importance in advanced atomic clock design, due to the naive expectation that the Q of a Cs gas cell frequency standard

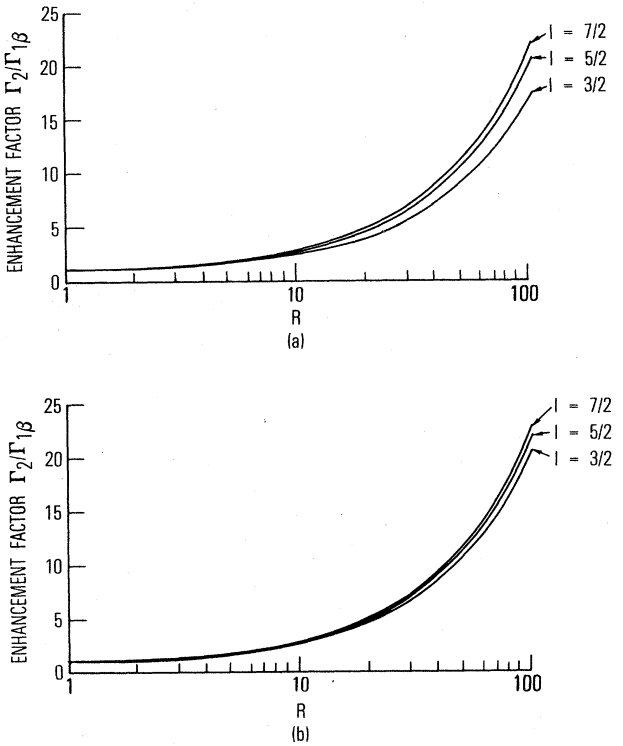

FIG. 2. The linewidth enhancement factor $\Gamma_2/\Gamma_{1\beta}$ as a function of the normalized photon absorption rate R ($R=B/\gamma$; $\gamma_1=\gamma_2$) for several values of the nuclear spin. (a) and (b) correspond to optical excitation out of the upper and lower ground-state hyperfine multiplets, respectively.

should be greater than the Q of a ^{87}Rb gas cell frequency standard if the photon absorption rate, relaxation rate, and Rabi frequency are equivalent in the two cases; this expectation is based on the fact that the Q is proportional to the resonant frequency of the 0-0 hyperfine transition. However, since gas cell frequency standards normally operate with some degree of power broadening,[12] one might actually expect the reverse to be true given the predictions of the present theory.

(iii) The LEF is an increasing function of the photon absorption rate and hence the optical-pumping laser intensity. Thus, the 0-0 linewidth depends on the light intensity in two distinct ways. The first is the well-known light broadening which arises through the dephasing rate Γ_2.[2] The second is an *"anomalous" light broadening* which is present even under conditions of extreme microwave power broadening. This latter is a direct consequence of the strong light-intensity dependence of the LEF.

(iv) Lastly, the LEF is a decreasing function of the relaxation rate γ, which implies rather odd behavior for the 0-0 linewidth. For example, assume that the 0-0 transition is initially power broadened and that $R \gg 1$. As the relaxation rate γ increases, the linewidth will exhibit *"anomalous" relaxation narrowing* because of the reduction of the LEF. However, as γ grows larger the linewidth will no longer be power broadened, but will instead be primarily determined by the dephasing rate Γ_2 which is an increasing function of the relaxation rate γ. This narrowing-to-broadening behavior in the dependence of the linewidth on the relaxation rate γ is illustrated in Fig. 3.

III. EXPERIMENT

From the preceding discussion it is clear that a crucial test for the generalized Vanier model lies in the predicted anomalous behavior of the power-broadened linewidth. Therefore, we decided to perform an experiment to verify the existence of anomalous light broadening in the 0-0 hyperfine transition of ^{87}Rb and to see if this anomalous light broadening was consistent with the theoretical predictions. To this end, the experiment proceeded through three separate phases. In the first phase we measured the amplitude of the 0-0 hyperfine transition as a function of microwave Rabi frequency. According to Eq. (21) and the two-level-atom approximation the amplitude should saturate in the microwave power-broadening regime. Thus, this phase of the experiment qualitatively indicated our ability to obtain sufficiently high microwave power. As evidence of our ability to power broaden the linewidth, and as a test of our experimental arrangement, the second phase of the experiment concerned the linewidth of the 0-0 transition as a function of microwave Rabi frequency: according to Eq. (23) and the two-level-atom approximation, the power-broadened linewidth of the 0-0 hyperfine transition should be a linear function of the Rabi frequency. Only with the successful completion of these first two phases did we proceed to the third and last phase, which was the observation of anomalous light broadening: operating with full microwave power, we measured the linewidth of the 0-0 transition as a function of optical-pumping light intensity. According to Eqs. (23) and (24), if the Vanier model's LEF had physical significance, we would observe a relatively large decrease in the power-

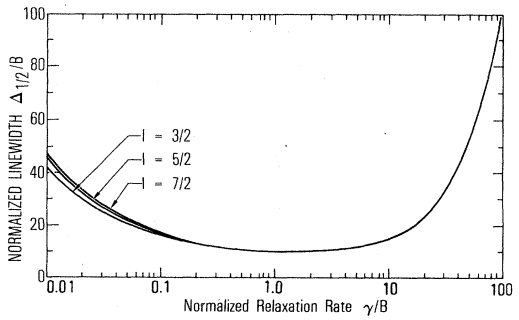

FIG. 3. The normalized linewidth $\Delta_{1/2}/B$ as a function of the normalized relaxation rate γ/B ($\gamma_1=\gamma_2$); optical excitation is out of the upper ground-state hyperfine multiplet, and $\omega_1/B=10$. For $\gamma/B<1$ the figure shows the phenomenon of "anomalous" relaxation narrowing for several values of the nuclear spin.

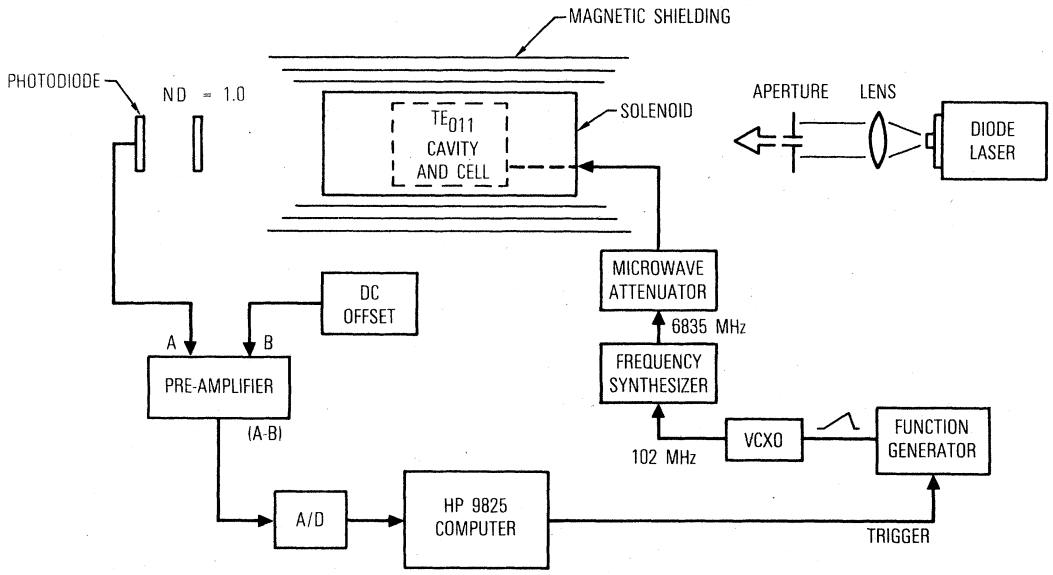

FIG. 4. Schematic diagram of the experimental arrangement discussed in the text.

broadened linewidth as the light intensity was reduced. If the two-level-atom approximation was correct, there would only be a slight, if any, change in the linewidth.

The experimental apparatus is shown schematically in Fig. 4. A Corning 7070 glass absorption cell which contained an excess of ^{87}Rb metal and 10-Torr N_2 was situated in a TE_{011} cylindrical microwave cavity ($L=5$ cm, $r_c=2.8$ cm) tuned to the ^{87}Rb ground-state hyperfine transition frequency 6835 Mhz; the cell filled the entire cavity. The N_2 was present in order to quench the Rb fluorescence and act as a buffer to reduce the effect of collisions with the cell walls. A static magnetic field of a few hundred milligauss was applied parallel to the cavity axis in order to define the quantization axis and to split the Zeeman levels so that only the 0-0 transition was induced by the microwaves. The cavity and cell were thermostatically controlled to ± 0.1 °C at about 37 °C and surrounded by three layers of magnetic shielding.

A single-mode AlGaAs diode laser, Mitsubishi ML-4101, tuned to the D_1 absorption line at 794.7 nm, was used to optically pump atoms from the $5^2S_{1/2}(F=2)$ hyperfine multiplet into the $5^2S_{1/2}(F=1)$ hyperfine multiplet; the laser intensity entering the absorption cell was 0.42 mW/cm^2. The Doppler-broadened absorption linewidth (~ 500 MHz) was greater than both the laser linewidth (60 MHz) and the Zeeman splitting (<700 kHz). Thus, optical pumping occurred from only the $F=2$ hyperfine state, but from all Zeeman sublevels of that state. Due to the combined effect of Doppler and pressure broadening, the excited-state hyperfine splitting was barely resolved.

The diode laser emission was collimated by a short-focal-length lens to a diameter of ~ 0.8 cm so that an aperture (~ 0.3 cm diameter) allowed only the central portion of the laser beam to enter the absorption cell. Defining the optical depth τ_d^{-1} by $I=I_0\exp(-\tau_d z)$, where I_0 is the incident light intensity and z is the axial position within the absorption cell, we measured $\tau_d^{-1}=7.6$ cm.[13] Thus, since the radial profile of the laser emission is well approximated by a Gaussian, and since the vapor was optically thin, the intensity distribution in the cell volume was expected to be fairly uniform. These precautions were necessary in order to reduce the effects of light-induced inhomogeneous broadening.[14]

The microwave frequency sweep was generated by applying a voltage ramp to a calibrated voltage controlled crystal oscillator (VCXO), whose output at ~ 102 MHz was multiplied up to the ^{87}Rb hyperfine frequency region. Placing precision microwave attenuators in the microwave transmission line allowed us to reduce the microwave power entering the cavity in a controlled fashion. Since the microwave power entering the cavity is proportional to the stored energy in the cavity, reducing the microwave power by precision attenuators resulted in a well-defined decrease in the microwave Rabi frequency. A single voltage ramp was initiated by a trigger pulse from a Hewlett-Packard HP 9825 computer, which also served as a signal averager. As the microwave frequency swept through the 0-0 hyperfine transition, the change in the transmitted laser intensity was detected with a Si photodiode and digitized for computer storage by an analog-to-digital converter. Care was taken to be sure that the passage through resonance was slow, since fast passage can influence both the signal amplitude and line shape.[15,16] All line shapes used in the data analysis represented a signal average of 100 passages through resonance.

Due to the presence of the buffer gas, the Rb atoms were essentially frozen in place in the cavity.[14] Thus, the microwave Rabi frequency experienced by a particular atom was determined by its spatial position within the

cavity mode. For a TE_{011} mode, the spatial variation of the microwave Rabi frequency is given by[17]

$$\omega_1(r,z)=\omega_{1p}\left|J_0\left[3.832\frac{r}{r_c}\right]\sin(\pi z/L)\right|, \quad (25)$$

where r is the radial position and ω_{1p} is the peak Rabi frequency. Since the laser beam was centered in the cavity and had a radius much less than the cavity radius, the spatial variation of the Rabi frequency for those atoms probed by the laser was well approximated by

$$\omega_1(0,z)=\omega_{1p}\sin(\pi z/L) . \quad (26)$$

Furthermore, for the low laser intensities used in the present experiment, the greatest contribution to the microwave resonance signal came from those atoms furthest from the cell wall (i.e., $z\simeq L/2$).[15,18] Thus, the Rabi frequency corresponding to our power-broadened linewidth was primarily determined by ω_{1p}. This expectation was tested experimentally by comparing the resonance linewidth at full microwave power and very low light intensity (LEF$\sim$1) with the peak Rabi frequency measured by the adiabatic rapid passage (ARP) technique.[19] The results were in excellent agreement, being, respectively, $\omega_{1p}(\mathrm{ARP})=(1.9\pm0.2)$ kHz and $\Delta_{1/2}=(2.00\pm0.08)$ kHz.

In Figs. 5 and 6 we show, respectively, the resonance signal's normalized amplitude and linewidth as a function of normalized Rabi frequency. The results clearly show that at the highest microwave power levels obtained the resonance line shape was power broadened and in qualitative agreement with both the two-level-atom approximation and the generalized Vanier model. We note that the intercept in Fig. 6 does not represent a residual linewidth in the limit of zero Rabi frequency; rather, it is taken as indicative of the scatter in the linewidth measurements.

To verify the existence of anomalous light broadening, we measured the linewidth of the 0-0 transition at full microwave power as a function of light intensity by placing neutral density (ND) filters in the laser beam path. A representative sample of the power-broadened line shapes for ND=0, 0.3, and 1.0 is shown in Fig. 7, and the functional dependence of the linewidth on light intensity is illustrated in Fig. 8. It is clear from both figures that there is a relatively large change, on the order of 100%, in the microwave power-broadened linewidth for the experimentally accessible range of light intensities.

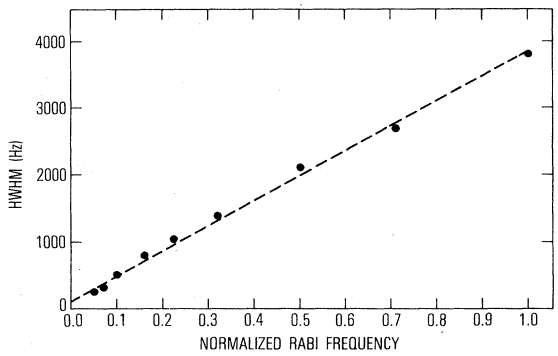

FIG. 6. Experimental measurements of the linewidth of the 0-0 hyperfine transition as a function of normalized Rabi frequency. The linearity of the data points is a clear indication that the linewidth is power broadened. The intercept does not indicate a residual linewidth; rather, it is indicative of the scatter of the data points.

IV. DISCUSSION

In order to compare theory and experiment quantitatively, it is necessary to know R for at least one value of the light intensity, since this quantity uniquely determines the LEF through Eq. (24). Similarly, from the measured linewidth at full light intensity, Eqs. (23) and (24) can be used to fit the theory to one experimental point. Since we had independently determined the Rabi frequency to be $\sim$2 kHz, Eq. (23) resulted in a full light-intensity LEF: $\Gamma_2/\Gamma_{1\beta}=3.6$. This LEF in turn implied a value for the normalized photon absorption rate at full light-intensity R_0 equal to 16. Thus, the solid curve in Fig. 8 was generated by reducing this value of R_0 appropriately, and as can be seen the agreement of this one-point theoretical fit

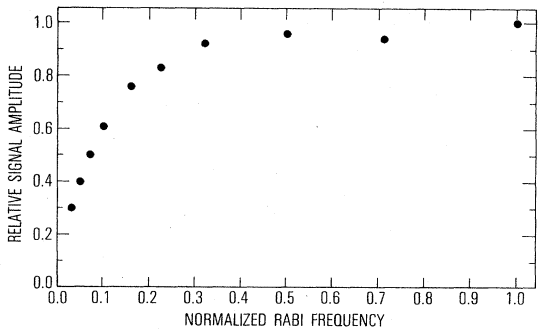

FIG. 5. Experimental results of the relative signal amplitude of the 0-0 hyperfine transition, pumping out of the $F=2$ hyperfine multiplet. Saturation of the signal amplitude is quite clear.

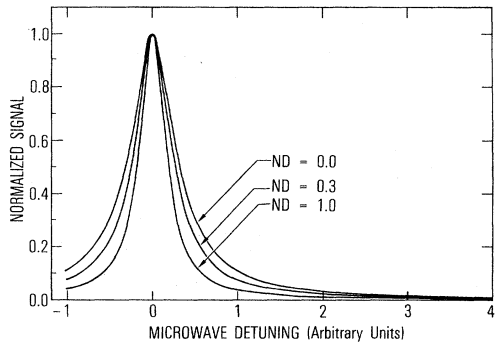

FIG. 7. A sample of the experimental full microwave power-broadened line shapes for three different light intensities; neutral density = 0.0, 0.3, and 1.0. "Anomalous" light broadening is readily apparent.

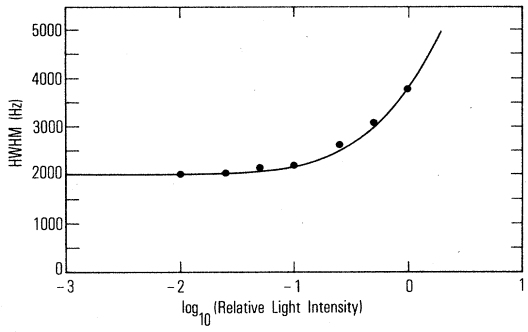

FIG. 8. The full microwave power-broadened linewidth as a function of relative light intensity. The dots correspond to experimental data; the solid line is a theoretical curve fit to the full light-intensity experimental point.

with the measured linewidths is excellent.

As a check on the theory, we can verify that the value of R_0 obtained with the theoretical fit is physically reasonable. Since $R_0=B_0/\gamma$, this can be accomplished by obtaining estimates of the full light-intensity photon absorption rate and the relaxation rate γ. From our measured values of the laser intensity and linewidth, it is straightforward to compute B_0:

$$B_0=\int \Phi(\nu-\nu_0)\sigma(\nu-\nu_0)d\nu \ , \tag{27}$$

where $\Phi(\nu-\nu_0)$ is the spectral density of the diode laser tuned to resonance (the spectral profile of the laser is Lorentzian), and $\sigma(\nu-\nu_0)$ is the absorption cross section for a photon of frequency ν. The photon absorption rate was evaluated numerically, since it was necessary to include natural, pressure and Doppler broadening into the absorption line shape. The calculation resulted in $B_0=740\ \mathrm{s}^{-1}$.

The calculation of the relaxation rate γ is actually fairly difficult, because the diffusion of optically pumped atoms to the cell walls, where they relax, is included phenomenologically into the density matrix rate equations; rigorously, a term $D\nabla^2\rho$ should have been included in Eq. (5),[6] where D is the diffusion coefficient for Rb atoms in N_2.[20] We therefore imagine that relaxation is composed of two terms: a bulk relaxation rate γ_0 representing spin exchange and buffer-gas collisions and a diffusional relaxation rate γ_d. Furthermore, we assumed that the diffusional relaxation rate could be described by some characteristic length r_s for the hyperfine polarization distribution in the cell (i.e., we imagine a sheath of polarization of radius r_s surrounding the laser beam[18]). The diffusional relaxation rate can then be approximated by $\gamma_d=D/r_s^2$, and therefore we have

$$\gamma=\gamma_0+\gamma_d=[\mathrm{Rb}]\bar{v}\sigma_{\mathrm{ex}}+[\mathrm{N_2}]\bar{v}\sigma_{\mathrm{bg}}+D/r_s^2 \ , \tag{28}$$

where [Rb] and [N_2] are the densities of rubidium atoms and nitrogen molecules, respectively, and σ_{ex} and σ_{bg} are the relaxation cross sections for spin exchange[21] and buffer-gas collisions,[20] respectively.[22]

Minguzzi *et al.*[18] have considered the spatial distribution of polarization in optical-pumping experiments for a step function radial light-intensity distribution. They find that the spatial distribution of polarization in a cylindrical cell can be written as a sum of diffusion modes:

$$P(r,z)=\sum_{i,\nu} A_{i\nu}J_0(\mu_i r/r_c)\sin(\pi\nu z/L) \ , \tag{29}$$

where μ_i is the ith zero of the zero-order Bessel function and $A_{i\nu}$ determines the amplitude of the mode. Using the parameters of the present experiment we find that a reasonable approximation is to ignore all terms other than those with $\nu=1$ and to consider only the first six Bessel functions:

$$P(r,z)\sim\sin(\pi z/L)\sum_{i=1}^{6} A_{i1}J_0(\mu_i r/r_c) \ . \tag{30}$$

As a crude approximation, then, we can estimate r_s as the radial position where the sum over the Bessel functions has dropped to one-half its value at $r=0$ and in this way obtain $r_s\sim 0.8$ cm. Using this value of r_s in Eq. (28) we find that $\gamma\sim 32\ \mathrm{s}^{-1}$, which results in $R_0\sim 23$. Thus, our experimentally determined value of R_0 is physically reasonable.

The above discussion clearly shows that the generalized Vanier model is quantitatively consistent with the experimental measurements. The question remains, however, as to a two-level atom's ability to show similar behavior. Obviously, if one made the additional assumption of short-duration collisions, so that $\gamma_1=\gamma_2$, the two-level-atom approximation would be in grave difficulty. Under this condition the two-level atom's linewidth becomes $\Delta_{1/2}=[(1/T_2)^2+\omega_1^2]^{1/2}$, so that the maximum light-intensity-related change in the power-broadened linewidth is $B_0^2/8\omega_1^2$. Since $B_0/\omega_1\sim 0.06$, this model can only give rise to a $\sim 0.04\%$ increase in the linewidth, and this is clearly contradicted by the experimental data.

One could, however, still choose to use the linewidth formula obtained with the two-level-atom approximation, but with more realistic values of T_1 and T_2. In this case T_1/T_2 would not necessarily be unity,[5] and one might expect to predict a more sensitive dependence of the power-broadened linewidth on light intensity. To make a fair comparison between this modified two-level-atom approximation and the generalized Vanier model, we will assume that the optical-pumping conditions are the same as those used in the calculation of the generalized Vanier-model line shape: no repopulation pumping, equal optical excitation rates from all Zeeman sublevels, and equivalent diffusional contributions to γ_1 and γ_2. Furthermore, since the phenomenological relaxation is dominated by diffusion ($\gamma_d\sim 23\ \mathrm{s}^{-1}$) we are justified in neglecting the effects of both spin exchange and buffer-gas collisions. With these considerations the LEF for the modified two-level-atom approximation is

$$\frac{T_1}{T_2}\simeq\frac{4B+8\gamma_d}{3B+8\gamma_d} \ . \tag{31}$$

Equation (31) predicts that the LEF saturates at high light intensities, and that the maximum enhancement in the power-broadened linewidth is only 16%. Both of these predictions contradict the experimental data. Thus,

there is no simple way to make the two-level-atom approximation consistent with experiment; however, even if there were, one would be faced with the task of justifying the *ad hoc* assumption of using realistic longitudinal and transverse relaxation rates in a two-level-atom model.

V. SUMMARY

We have shown that one cannot adequately describe the 0-0 hyperfine line shape in optically pumped alkali-metal vapors with a two-level-atom approximation. Specifically, the effect of the nuclear spin, manifested in the different degeneracies of the two hyperfine sublevels, results in a power-broadened linewidth that can be orders of magnitude greater than the Rabi frequency. Furthermore, when the power-broadened linewidth is properly analyzed, both anomalous relaxation narrowing and anomalous light broadening are predicted. In the present work the latter was experimentally observed and compared with the theoretical prediction.

To conclude, we note somewhat parenthetically that Bhasker *et al.*[23] have recently observed power-broadening enhancement in some optical-pumping experiments on Cs. Their LEF, however, was fundamentally different from the one discussed above, since it arose from a physical distinction between longitudinal and transverse relaxation rates in the presence of rapid spin exchange. The enhancement factor under discussion here is more statistical than physical in origin, though the anomalies associated with the linewidth are just as striking.

ACKNOWLEDGMENTS

This work was sponsored by the United States Air Force Space Division under Contract No. F04701-83-C-0084.

[1]W. E. Bell and A. L. Bloom, Phys. Rev. **107**, 1559 (1957).
[2]A. Kastler, J. Opt. Soc. Am. **53**, 902 (1963).
[3]For this predominantly illustrative introduction we have assumed that spin-exchange effects are negligible. Actually, it has been shown (see Ref. 8) that for the 0-0 hyperfine transition, the dephasing rate due to spin exchange is slower than the longitudinal relaxation rate due to spin exchange. Thus, under certain conditions one could expect $T_1 < T_2$, which would imply that T_1/T_2 was a linewidth reduction factor.
[4]D. Pines and C. P. Slichter, Phys. Rev. **100**, 1014 (1955).
[5]A. L. Bloom, Phys. Rev. **118**, 664 (1960).
[6]W. Happer, Rev. Mod. Phys. **44**, 160 (1972).
[7]H. Kopfermann, *Nuclear Moments* (Academic, New York, 1958), pp. 4—71.
[8]J. Vanier, Phys. Rev. **168**, 129 (1968).
[9]G. Missout and J. Vanier, Can. J. Phys. **53**, 1030 (1975).
[10]F. A. Franz, Phys. Rev. **141**, 105 (1966).
[11]B. S. Mathur, H. Tang, and W. Happer, Phys. Rev. **171**, 11 (1968).
[12]L. G. Bernier, A. Brissom, M. Tetu, J. Y. Savard, and J. Vanier, in *Proceedings of the 34th Annual Symposium on Frequency Control, Philadelphia, 1980* (Electronic Industries Association, Washington, D. C., 1980), pp. 376—383.
[13]The optical depth was measured with very low light intensity so that there was no optical pumping (i.e., a neutral density filter of 3.0 was placed in the beam path).
[14]J. C. Camparo, R. P. Frueholz, and C. H. Volk, Phys. Rev. A **27**, 1914 (1983).
[15]J. C. Camparo and R. P. Frueholz, Phys. Rev. A **30**, 803 (1984).
[16]P. R. LeFrere and D. C. Laine, Phys. Lett. **41A**, 93 (1972).
[17]J. D. Jackson, *Classical Electrodynamics* (Wiley, New York, 1975), pp. 353—356.
[18]P. Minguzzi, F. Strumia, and P. Violino, Nuovo Cimento **46B**, 175 (1966).
[19]R. P. Frueholz and J. C. Camparo, J. Appl. Phys. (to be published).
[20]F. A. Franz and C. Volk, Phys. Rev. A **14**, 1711 (1976).
[21]N. W. Ressler, R. H. Sands, and T. E. Stark, Phys. Rev. **184**, 102 (1969).
[22]We note that the mechanisms of spin exchange and buffer gas collisions do not represent true uniform relaxation, though this is how they are incorporated into the theory. However, it is not clear that a more rigorous description of the relaxation processes is necessary at the present time for an adequate description of the 0-0 line shape.
[23]N. D. Bhasker, J. Camparo, W. Happer, and A. Sharma, Phys. Rev. A **23**, 3048 (1981).